ISSN 0001-4370, Oceanology, 2021, Vol. 61, No. 1, pp. 1–14. © Pleiades Publishing, Inc., 2021.
Russian Text © The Author(s), 2021, published in Okeanologiya, 2021, Vol. 61, No. 1, pp. 5–20.

MARINE PHYSICS

Hydrophysical Structure and Current Dynamics of the Kodor River Plume

A. A. Osadchiev[a, *], A. A. Barymova[b], R. O. Sedakov[a, c], A. V. Rybin[c], A. G. Tanurkov[c], A. A. Krylov[a, c], V. V. Kremenetskiy[a], S. A. Mosharov[a, d], A. A. Polukhin[a], A. S. Ulyantsev[a], M. A. Osadchiev[a], and R. S. Dbar[e]

[a] *Shirshov Institute of Oceanology, Russian Academy of Sciences, Moscow, Russia*
[b] *Marine Research Center at Moscow State University, Moscow, Russia*
[c] *Moscow Institute of Physics and Technology, Dolgoprudny, Russia*
[d] *Bauman Moscow State Technical University, Moscow, Russia*
[e] *Azov-Chernomorsky branch of the FSBSI "VNIRO" ("AZNIIRKH"), Rostov-on-Don, Russia*
**e-mail: osadchiev@ocean.ru*

Received February 10, 2020; revised August 5, 2020; accepted August 15, 2020

Abstract—This work is focused on the river plume generated by the Kodor River which is the largest river of Abkhazia and the northeastern coast of the Black Sea. Based on in situ hydrological data, quadcopter aerial images and satellite observations, hydrophysical structure and circulation in the Kodor plume was studied at different river discharge conditions. Discharge of the Kodor River, which inflows to sea from several deltaic branches forms a relatively shallow plume with large area, as compared to the Mzymta River, the largest estuarine river of the study region, at similar hydrological, meteorological, and oceanographic conditions. Due to its small vertical size and large salinity gradient at the border with the subjacent saline sea, the Kodor plume is characterized by quick response on wind forcing variability. The Kodor plume also has large spatial inhomogeneity, caused by its formation conditions (several closely located freshwater sources prone to abrupt discharge variability), as well as regional bathymetry (interaction between the plume and shoals). During low discharge period, the inflowing Kodor River has relatively low kinetic energy, which causes abrupt deceleration of the jet in the sea area adjacent to the river mouth. As a result, the inertia of the inflowing jet abruptly decreases and large velocity and salinity gradients are formed in vicinity of river estuary, which hinder formation of anticyclonic circulation at the near-field part of the plume. This feature induces transport of freshwater discharge off the river mouth and its accumulation in the far-field part of the small plume under moderate wind forcing conditions that is not typical for large river plumes. The obtained results are important for understanding general aspects of dynamics of buoyant plumes formed by rivers with small discharge rates.

Keywords: river plume, coastal circulation, continental runoff, wind forcing, Black Sea, Kodor River
DOI: 10.1134/S000143702101015X

1. INTRODUCTION

Significant continental runoff, about 30 km^3 annually [3], enters the Black Sea from the Republic of Abkhazia. Less than half of this amount is provided by several large rivers: Kodor (4.2 km^3), Bzyb (3.8 km^3), Ingur HPP discharge channel (3.2 km^3), Ingur (1.2 km^3), and Gumista (1.1 km^3) (Fig. 1). Most of the total continental runoff from Abkhazia enters the Black Sea from more than 30 small rivers, the catchment areas of which are located in numerous gorges at the southern part of the Main Caucasus Range and do not exceed 500 km^2 in area.

Abkhazia occupies only 5% of the Black Sea coastline, while freshwater runoff from Abkhazia constitutes 8–10% of the total freshwater runoff into the Black Sea [2, 3]. Thus, the role of freshwater runoff in the hydrological structure and dynamical processes in this region is significantly higher than on the average in the Black Sea. These processes are particularly pronounced during the periods of spring–summer freshet and short-term autumn rainfall floods when increased runoff of numerous rivers along the Abkhazian coast form freshened water masses, which significantly affect the structure and dynamics of the coastal zone (Fig. 2).

Regular oceanographic measurements in the Abkhazian coastal sea zone were actively performed until the early 1990s, which resulted in a relatively good study of the general structure of the coastal zone in areas with inland runoff inflow according to the standards of those years. Nevertheless, measurements by novel methods and instruments in this region have not been performed for the past 30 years, studies in the coastal zone of Abkhazia were limited to occasional

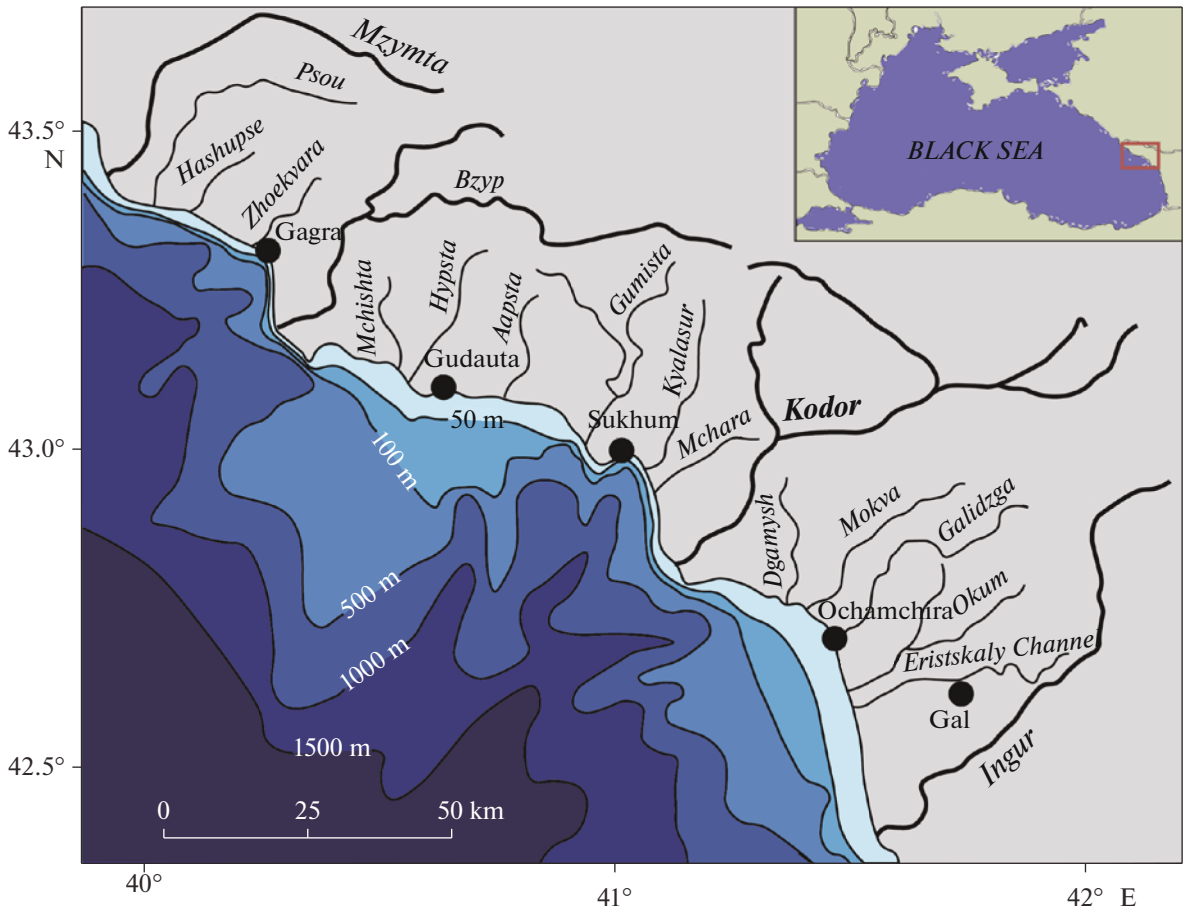

Fig. 1. Major rivers, towns, and bottom topography of Abkhazian sector of Black Sea coast. Kodor River is marked in boldface.

monitoring measurements. During this period, there were significant changes in the temperature regime and annual rainfall amounts recorded at meteorological stations of the Republic of Abkhazia compared to the situation in the 1950s–1980s. As a result, the modern influence of the Abkhazian river runoff on the structure and dynamics of the coastal zone has hardly been investigated at all. In the recent scientific literature, there are only single cases and rather limited data on these processes [8, 11, 12], which have certain socioeconomic and recreational importance for the Republic of Abkhazia.

Studies of plumes formed by small rivers in Abkhazia are also of fundamental importance in context of studying the general aspects of dynamics of small river plumes. The transformation of freshwater continental runoff as a result of its interaction with seawater can be considered and analyzed on various spatial and temporal scales. Initially, river runoff enters the sea from the mouth and forms a submesoscale or mesoscale water mass, called a river plume, which salinity is much lower than that of the surrounding seawater. The buoyancy force plays an important role in the distribution and mixing of this freshened water mass, so the dynamics of river plumes and surrounding seawater are different due to differences in salinity [40, 43]. Salinity is thus the main characteristic used to distinguish river plumes from seawater, i.e., to determine the mixing zone where the river plume ends and seawater begins.

A river plume is generally formed by one or more distinct sources of freshwater runoff. The structure and dynamic characteristics within a river plume are significantly heterogeneous. In particular, salinity and flow velocity fields in the plume near a freshwater source(s) and in the outer part of the plume differ significantly [16, 21, 27, 33, 34]. A river plume spreads and mixes with the surrounding seawater, which, on the one hand, leads to its transformation and, on the other hand, affects the physical, biological, and geochemical characteristics of the surrounding seawater. The degree and spatial scale of these effects mainly depend on the volume of freshwater runoff and vary from insignificant effects of small river plumes formed by rivers with small runoff volumes [5, 24, 42–45, 49, 53] to the formation of freshened water masses in the surface layer of the sea on wide coastal and shelf areas [9, 14, 17, 35, 38, 39, 41, 47, 48, 52]. These water masses, also called ROFI's, are characterized by a

Fig. 2. Numerous river plumes along coast of Abkhazia and longshore freshened zones during spring flood on April 6, 2018, visible on Landsat 8 optical band satellite image.

more homogeneous structure, significantly larger spatial scales, and lesser temporal variability compared to river plumes.

We consider river plumes as water masses resulting from the transformation of freshwater runoff in the coastal zone on on time scales from daily to mesoscale, and ROFI's as a result of transformation of freshwater runoff on time scales from seasonal to annual. River plumes enclosed in ROFI's are a continuous process of freshwater runoff transformation and thus cannot be clearly separated. On the other hand, river plumes and ROFI's have very different thermohaline and dynamic properties. Therefore, the interaction of river plumes and surrounding ROFI's significantly affects the dynamics of propagation and mixing of river plumes on mesoscale time scales [23, 34, 36, 37, 46].

This article addresses small river plumes, so it is necessary to define the characteristics of small river plumes that distinguish them from large ones: small river plumes do not form ROFI's; i.e., the residence time of freshened water in a small river plume runs from hours to days (43). Dissipation of freshened water when a small plume mixes with the underlying seawater barely affects the surrounding seawater and does not lead to accumulation of freshwater runoff in adjacent areas of the sea. As a result, small plumes are characterized by significant salinity and density gradients at their interfaces with surrounding seawater. These density gradients prevent vertical energy exchange between the small plume and the underlying seawater.

This property strongly affects the small plume dynamics as follows. First, most of the wind energy transferred to the sea remains in the small plume, as the vertical energy flux decreases significantly at the density gradient between the plume and the underlying seawater layer. Thus, the frictional stress of the wind is concentrated in a narrow freshened surface layer, which leads to higher motion velocities and a faster response of the small plume dynamics to variability of wind action compared to the surrounding water [6, 7]. Second, the circulation in the surround-

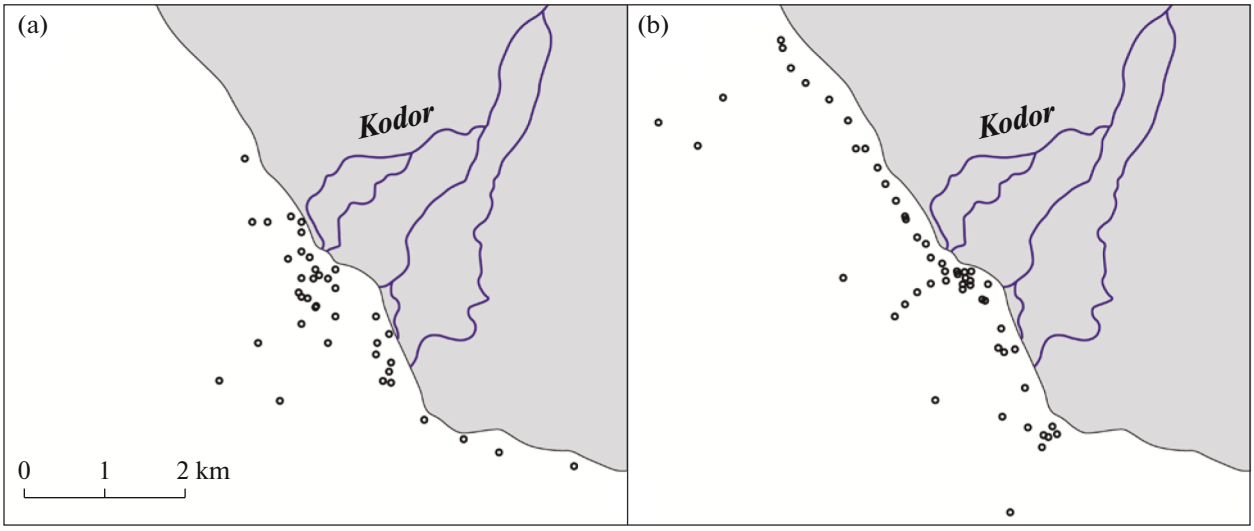

Fig. 3. Location of hydrological stations around distribution of Kodor plume on August 29–September 2, 2018 (a) and April 1–4, 2019 (b).

ing seawater has little effect on the small plume dynamics because the density gradient prevents vertical energy flux from the underlying seawater layer to the small plume [42]. As a result, the small plumes dynamics are primarily determined by the wind, which leads to very high temporal variability of their locations, shapes, and areas [31, 32, 40, 53]. The type of small plume propagation can change drastically within a few hours, which is regularly recorded by in situ measurements and satellite observations. The high spatial and temporal variability of small plumes and their small vertical sizes often result in great inhomogeneity of their horizontal structure.

2. STUDY AREA AND DATA USED

The Kodor is the largest river in Abkhazia and the entire northeastern Black Sea coast. The Kodor flows into the Black Sea 20 km south of Sukhum on a protruding stretch of coast between Sukhum and Skurcha bays. When flowing into the sea, the Kodor River forms a 10 km^2 delta artificially created in recent years as a result of the construction of additional delta channels, shore protection, and hydrotechnical facilities. The water regime of the Kodor River has a pronounced spring–summer flood and autumn–winter drought [1]. In addition, more than a dozen intensive but short-term instances of rainfall occur annually on the river, most of them in the autumn–winter period. Sharp rises and drops of water level during floods are caused by the large slope of the Kodor catchment area (up to 40°–60°), which occupies mountain gorges in the southern part of the Main Caucasus Range, and the high density of the river network, which leads to rapid inflow of rainwater into river channels. Due to the relatively small catchment area (about 2000 km^2) and the small length of the river (84 km), the discharge rate in the lower reaches of the Kodor and thus the volume of river runoff into the sea can increase dramatically within a few hours after the beginning of intensive precipitation.

The research on the Kodori plume is based on field data collected during two coastal expeditions to the adjacent Kodori River, conducted under different river runoff conditions: during a short-term rainfall flood from August 29 to September 2, 2018, and during the winter–spring low water period April 1–4, 2019. The expeditions were conducted on the small fishing vessels *Vladimir* and *Adygeets* and involved hydrophysical, hydrochemical, and hydrobiological studies. The present article considers and interprets the results of hydrophysical measurements, while its accompanying article is devoted to hydrochemical studies [10].

The in situ data used are continuous temperature and salinity measurements in the surface layer (at a depth of 1 m) along the ship track performed by a flow-through system equipped with a CTD instrument (Yellow Springs Instrument 6600 V2) [4, 5] and vertical temperature, salinity, and current velocity profiles measurements at hydrological stations, obtained with CTD-ADCP instrument (Aanderaa SeaGuard RCM) from August 29 to September 2, 2018, or a CTD instrument (Sea-Bird Electronics 19plus) from April 1 to April 4, 2019 (Fig. 3).

The expedition also used an unmanned aerial vehicle (a DJI Phantom 4Pro quadcopter). Its small size allows performing take-off and landing from the deck of a small ship. During flights, the key morphological zones and dynamic features of the river plume were photographed and videotaped for reconnaissance, observation of the river plume dynamics, selection of

hydrophysical work points, and vessel positioning. An experiment using floating drifters was also carried out to study the structure of surface currents in the nearshore zone of the river plume. Two series of drifters were launched into the Kodor River. The movement of drifters in the coastal zone from the moment they entered the sea was tracked by video footage from the quadcopter. Computer processing of the obtained video records made it possible to reconstruct the velocity and quadcopter trajectories of the plume currents in the near-mouth area.

The main meteorological characteristics (wind speed and direction, temperature, humidity, atmospheric pressure) were measured with a Gill GMX200 portable weather station. The weather station was installed at a height of 10 m on a pier near Cape Krasny Mayak (Sukhum) 30 n from shore, away from relief elevations, tall trees, and structures. The measurement resolution of meteorological characteristics was 1 min. In addition to raw data, satellite images of the studied region acquired by Landsat 8 OLI (http://earthexplorer.usgs.gov/) and Sentinel-2 MSI (https://scihub.copernicus.eu/) sensors were used in the study.

2. RESULTS

3.1. Hydrological structure of the Kodor plume. The hydrological structure of the Kodor plume was studied based on field data, satellite images, and quadcopter images. Salinity distributions of the sea surface layer, influenced by Kodor River runoff, were mapped from the field measurements. They give an idea of the thermohaline structure and spatial scale of the plume. Figure 4 shows the surface salinity distribution maps for August 31, September 1, and September 2, 2018, based on flow-through system measurements. Drone photography of the plume as part of the expedition made it possible to refine the spatial scale of the plume, study its small-scale internal structure, and short-period temporal variability (Fig. 5). Landsat 8 and Sentinel-2 satellite images of the studied region obtained during the expedition made it possible to compare images of the Kodor plume in the optical range with surface salinity distributions and the salinity and turbidity structures of the sea surface layer in the zone of influence of the Kodor River (Fig. 6). Subsequent analysis of optical Landsat 8 and Sentinel-2 images of the same region, taken in 2013-2019, made it possible to study mesoscale and seasonal variability of the Kodor plume to assess its response to fluctuations in runoff during the spring flood–summer low water period, as well as short-term autumn–winter floods.

The field thermohaline measurements showed that the Kodor plume is clearly characterized by a lower salinity (<15 PSU) compared to the salinity of the surrounding seawater (16–18 PSU, Fig. 4). The temperature in the plume was also lower than the seawater temperature due to the effect of snow and ice on water supply of the Kodor River [1]. The difference between the temperature of the surface layer of the sea and the plume was relatively small during the fieldwork at the end of the cold period of the year in April 2019 (0.5°C), but in August-September 2018 in the warm sea conditions it was significant 3–4°C. The outer limits of the areas of low temperature, low salinity and high turbidity in the surface layer correlate well with each other. When crossing the sharp front between the sea and the plume, the salinity of the surface layer fell sharply from 16–18 to 13–15 PSU at less than 5 m, which was accompanied by a drop in temperature and increased turbidity. Such sharp gradients testify to the small influence of the process of river plume mixing with salty seawater on thermal and optical properties of surrounding seawater. This situation is typical for plumes formed by small rivers in open coastal areas, for plumes of small rivers in the Russian part of the Black Sea coast. [5, 31, 42].

We compared the hydrological structure of the Kodor River plume with that of the Mzymta River, the largest estuarine river in the Russian part of the Black Sea coast, the mouth of which is 120 km northwest of the Kodor River delta. The Kodor and Mzymta plumes are formed under similar hydrological, meteorological, and oceanographic conditions. Marine measurements in these plumes were taken during periods of similar water runoff (100–150 m^3/s) and similar atmospheric action (wind <5 m/s). However, the spatial scale and salinity anomaly of the Kodor River plume was significantly higher than that of the Mzymta. Thus, the longshore length of the Kodor plume was 10–15 km, while the spatial extent of the Mzymta plume under similar external conditions did not exceed 3–5 km [5, 31, 37]. Surface salinity in the Kodor plume varied from 0–1 PSU at 100 m to 8–10 PSU at 2 km from the mouths of the delta channels (Fig. 4). Surface salinity in the Mzymta plume under similar conditions exceeded 6 PSU at 100 m and 14 PSU at 2 km from the mouth [5, 42].

The vertical scales of the Kodor and Mzymta plumes exhibit significant differences too. The thickness of the Kodor plume was 1.5–2.5 m over the entire plume area (Fig. 7a) except for narrow (tens of meters) areas along the outer boundaries of the plume (Fig. 7b). Measurements on April 3, 2019, showed that the plume thickness sharply increases to 4–6 m at 15–20 m from the sharp boundary of the plume and surrounding seawater (profiles *6*, *7* in Fig. 7b). At the same time, the plume thickness at 100 m from the plume boundary (profile *5* in Fig. 7b) was only 2 m. This seems to be caused by plume convergence and downwelling on the well-defined frontal boundary between the plume and the sea [25, 26, 30]. The thickness of the Mzymta plume, based on measurements of different years, was on average almost twice as large and decreased from 4–5 m in the downstream area to 2–3 m at the plume boundary [5, 37].

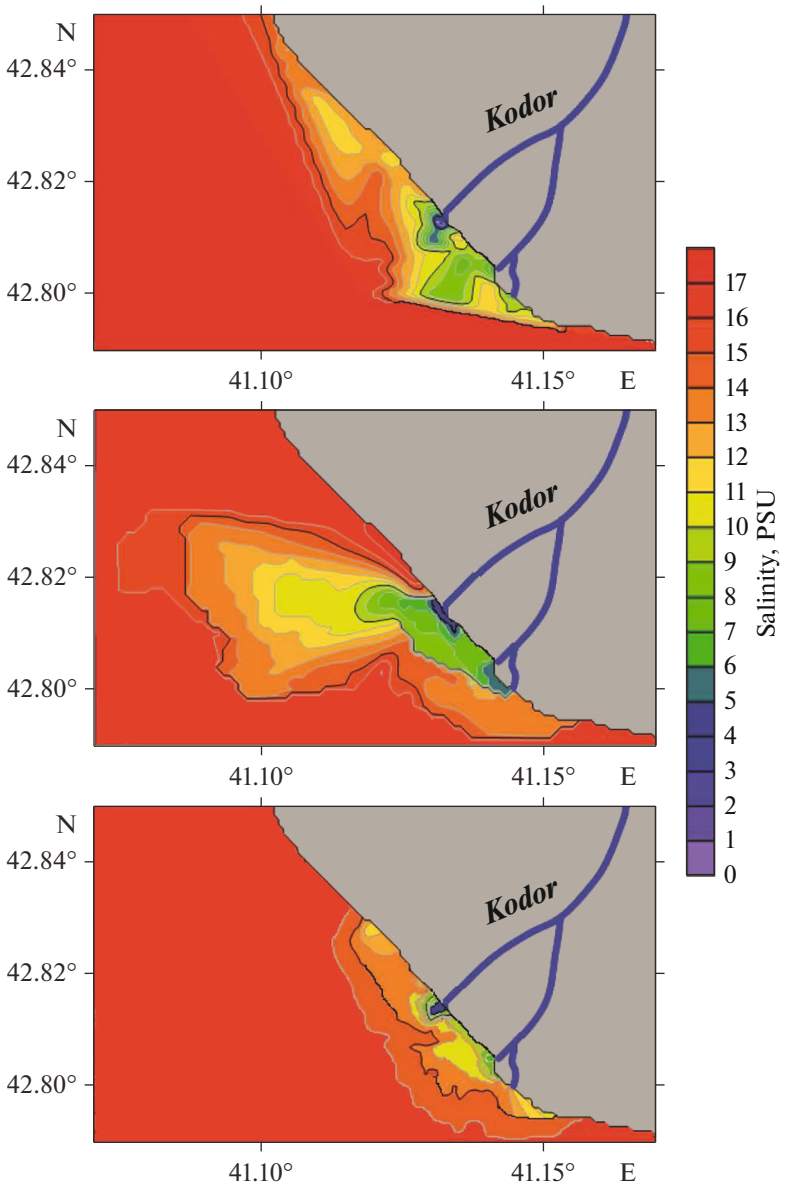

Fig. 4. Surface salinity distribution in zone of influence of Kodor river runoff on (a) August 31, (b) September 1, and (c) September 2, 2018.

Fig. 5. Aerial photos of southern part of Kodor plume taken on (a) September 1, 2018, (b) September 2, 2018, and (c) April 3, 2019. Arrow shows location of Cape Kodor.

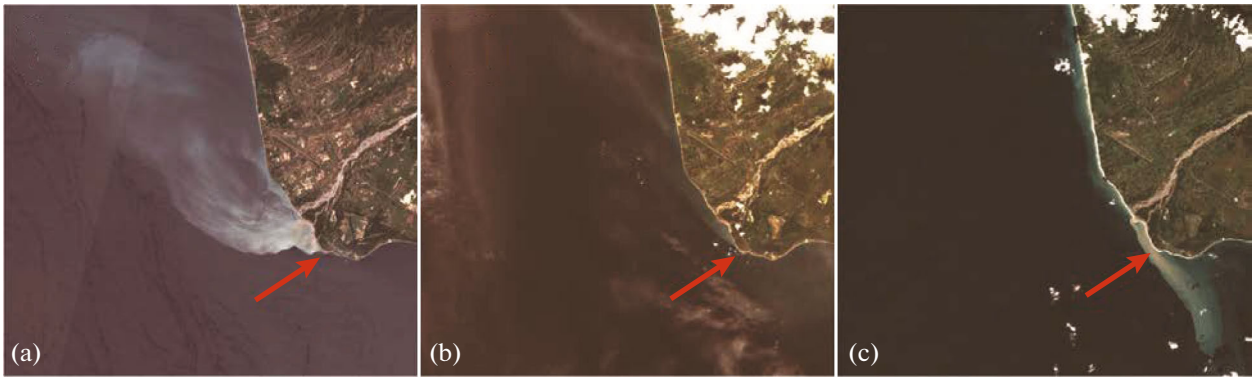

Fig. 6. Satellite images of Sentinel-2 of study area in optical range, taken on (a) June 27, (b) August 31, and (c) October 5, 2018. Arrow shows location of Cape Kodor.

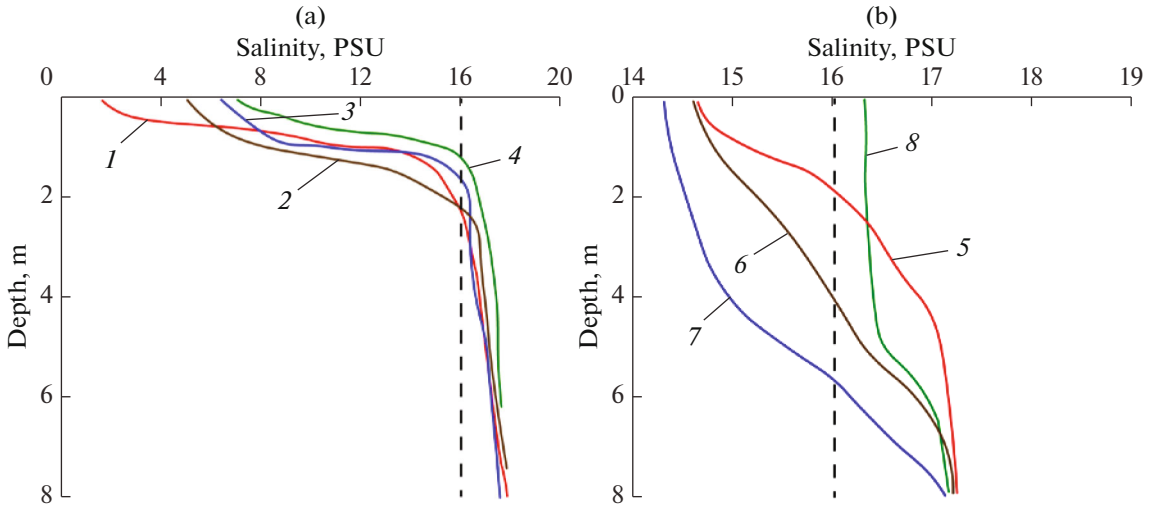

Fig. 7. Vertical salinity profiles in Kodor plume measured on (a) August 31, 2018, at distance of 200 (*1*, red), 300 (*2*, brown), 500 (*3*, blue), and 1100 m (*4*, green) from mouth of delta change; (b) April 3, 2019, in plume at distances of 100 (*5*, red), 15 (*6*, brown) and 1 m (*7*, blue) from plume boundary and in surrounding seawater at distances of 4 m from plume boundary (*8*, green). Dotted lines show location of conditional plume boundary (16 PSU isohaline).

Analysis of Landsat 8 and Sentinel-2 images for 2013–2019 confirmed that the area of the Kodor plume is on average several times larger than that of the Mzymta. One hundred eight-four satellite images of the Mzymta plume and 235 satellite images of the Kodor plume taken on different days allowed us to determine these plumes boundaries, based on the correspondence of turbidity and salinity gradients at the outer boundaries of these plumes [31, 42]. Based on these data, the average monthly and annual areas of Mzymta and Kodor plumes were calculated (Fig. 8). The annual runoff of the Kodor River (4.2 km^3) was 2.5 times larger than that of the Mzymta (1.6 km3) [3]. However, according to the satellite images, the average annual area of the Kodor plume (53.9 km^2) is more than four times that of the Mzymta (12.9 km^2). The average areas of the Kodor and Mzymta plumes during the spring flood (April–June), calculated from available cloudless satellite images, were 98.7 and 21.2 km^2, respectively. The impact of short-term autumn rainfall floods is also more pronounced in the Kodor plume than in the Mzymta. The average area of the Kodor plume during the flood season (September–November) is 32.3 km^2, while the average area of the Mzymta plume is only 11.7 km^2.

During the expedition, the response of the surface structure of the Kodor plume to a short-term flood event caused by a heavy rainfall on the night of August 31 to September 1, 2018 was studied. Rainwater flooding on the Kodor River lasted no more than 6 hours, but it had a significant impact on the river plume, which was recorded by contact measurements and aerial photography. The flood caused not only an increase in river discharge, but also was accompanied

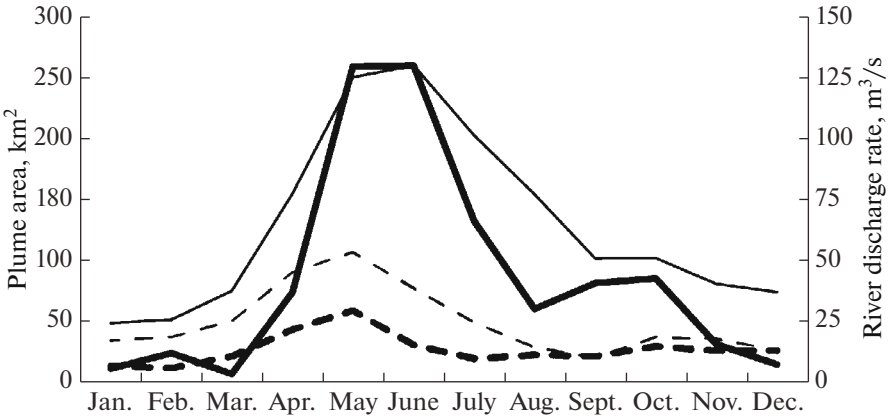

Fig. 8. Monthly average flow rate (thin lines) and areas (thick lines) of Kodor (solid lines) and Mzymta plumes (dashed lines). Plume areas were calculated from available uncloudy satellite Landsat 8 and Sentinel-2 images for 2013–2019.

Fig. 9. Aerial photos of adjacent part of Kodor plume taken on (a) August 31, (b) September 1, and (c) September 2, 2018.

by a sharp increase in the concentration of terrigenous suspended solids in river discharge. As a result, the turbidity of the Kodor plume immediately after the September 1 flood was significantly higher than before August 31 (Fig. 9). The spatial dimensions of the plume have also more than doubled compared to the preflood state (Fig. 4), while the thickness and salinity anomaly in the adjacent part of the plume remained virtually unchanged. Measurements taken on September 2 showed that a day after the short-term flood, the turbidity in the Kodor plume decreased to the preflood values (Fig. 9), but the plume area remained much larger (Fig. 4).

In contrast to most small river plumes [44, 45, 53], including those in the Russian sector of the Black Sea coast, the horizontal salinity distribution in the Kodor plume is extremely heterogeneous and has no direct relation to the distance to the nearest freshwater source, i.e., the mouth of the nearest delta channel. This seems to be the simultaneous result of several peculiarities in the formation and propagation of the Kodor plume. First, as mentioned above, during short-term rainfall floods, the area of the plume under study can change several times in less than a day. Because of this, the plume, which was formed earlier and did not have time to dissipate due to mixing with seawater, has significantly different thermohaline and dynamic characteristics compared to the plume that formed during the measurement. The residual and new plumes thus create a complex system of internal fronts and interact as separate water masses.

Second, the plume of the Kodor delta distributary is formed by several spatially separated freshwater sources. As a result, the coastal part of the Kodor plume is characterized by significant heterogeneity in the thermochaline characteristics, strongly pronounced in the obtained temperature and salinity maps (Fig. 4) and satellite and aerial photographs (Fig. 10). The areas of the Kodor plume adjacent to the mouths of the distributaries have different hydrophysical structures and dynamics and interact with each other as different water masses. Aerial photos show clear frontal zones between them (Fig. 4). Measurements taken on September 2, 2018, showed significant differences in salinity and temperature at a distance of less than 5 m to the north (14 and 27°C) and south (8–10 and 26°C) from such a frontal zone. Measurements of currents recorded significantly different dynamic characteristics in these water masses.

Fig. 10. Aerial photos of frontal zone (red arrows) between water masses of Kodor plume formed by adjacent delta channels, taken on (a) September 1, 2018, (b) September 2, 2018, and (c) April 3, 2019.

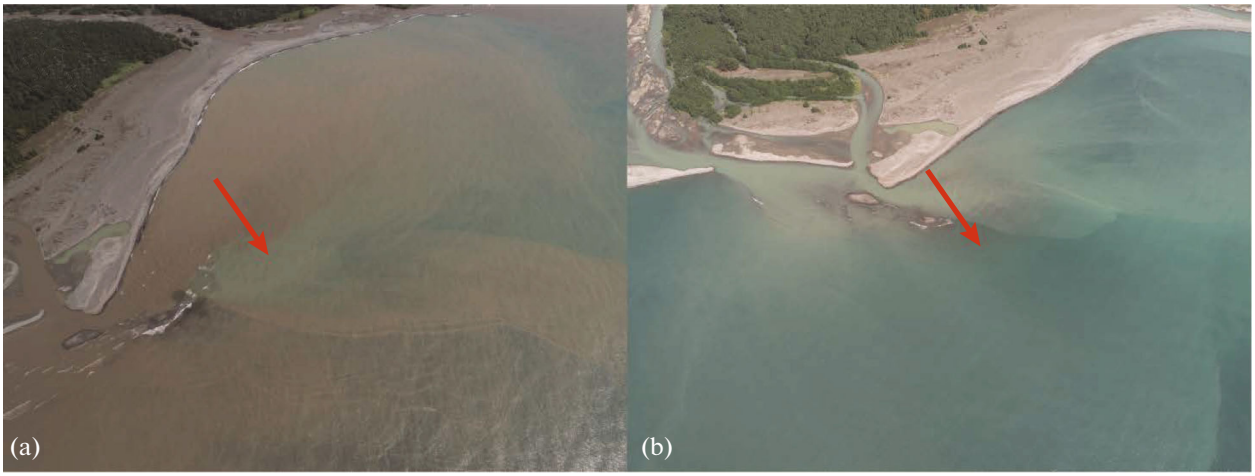

Fig. 11. Aerial photos of area of reduced turbidity and increased salinity (see red arrows) formed by flow of Kodor plume in shoal, taken on (a) September 1 and (b) September 2, 2018.

Third, the horizontal heterogeneity of the hydrophysical structure of the Kodor plume is caused by the interaction of incoming continental runoff with the features of the bottom topography in the coastal zone. Thus, in the Kodor plume, there was an zone of reduced turbidity that formed behind a shallow basin opposite one of the distributaries (Fig. 11). This was especially pronounced on the day after a rainfall flood, accompanied by increased plume water turbidity. This area was also characterized by higher salinity values, which was 3 PSU higher than that of the adjacent turbid plume area. The formation of this zone seems to have been caused by the dynamic effect of the river jet flowing around an obstacle and the shallow water depth behind the spit, slowing the velocity of the river plume.

3.2. Circulation in the Kodor plume. The expedition also studied certain circulation features of the Kodor plume. Measurements of vertical current profiles in the plume using the ADCP probe have shown that the current velocity and direction in the plume generally differs from that in the underlying seawater layer. Thus, on August 31, 2018, one of the stations in the plume (at a depth of 1.5–2.5 m) observed a easterly current with a speed of 0.2 m/s, and, in the lower seawater layer (at a depth of 3.5–4.5 m), there was a southerly current with a speed of 0.1 m/s. The presence of its own dynamics, different from that of the surrounding seawater, is typical of river plumes [21], including small river plumes in the Russian sector of the Black Sea coast [6, 7, 40].

During the expedition on September 1, 2018, a drone survey detected an anticyclonic eddy in the Kodor plume at its outer bounder (Fig. 12). The eddy was about 500 m in diameter; it moved northward at a speed of about 0.9 m/s and twisted at a rate of about 0.4 m/s. The eddy seemed to have formed by the longshore Cape Iskuria current, north of the Kodor delta. The eddy existed for about 1 h, after which it merged with the outer boundary of the plume and ceased to exist. Based on the aerial photographs, after the eddy dissipated at the outer boundary of the Kodor plume, an of internal wavepacket occurred in this section of the frontal zone (Figs. 12c, 12d). The propagation velocity of internal waves in the direction of the open sea was about 0.3 m/s, and the distance between waves

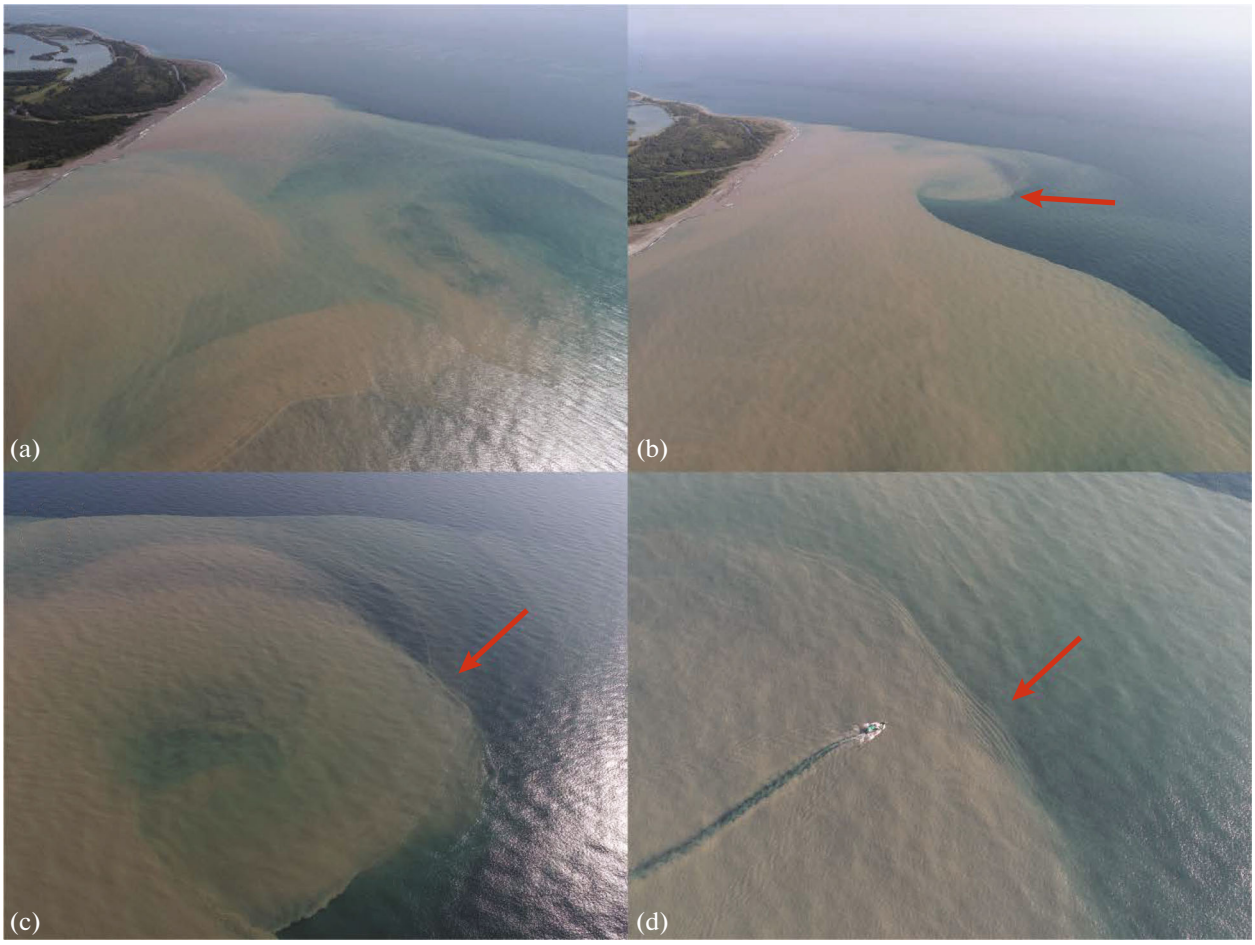

Fig. 12. Aerial photographs of southern part of Kodor plume 2.5 h before (a) and during (b) eddy formation (red arrow); aerial photographs of eddy (c) and inner wave packet separating it from its outer boundary (d) (red arrow), taken on September 1, 2018.

was 2–4 m. There were 12 waves with lengths of ~50 m in the central part of the wave train and only 3–4 waves with lengths of ~200 at its periphery. At about 500 m from the place of their formation, the internal waves dissipated and new internal waves did not form either here or in other parts of the frontal zone between the plume and the sea. Thus, we suggest that the source of internal wave formation was eddy dissipation in the plume and transfer of the eddy energy to the internal wave propagation energy.

On April 4, 2019, a drift experiment to study circulation in the adjacent part of the plume was conducted in the area where one of the Kodor distributaries flows into the sea. Ten drifters were launched into the surface layer of Kodor River 200 m from where the river enters the sea. The drifters were launched in two series of five apiece, and the time between launches of drifters in one series was 2 s; the time between the two series was 10 min. The trajectories of drifters in the coastal zone were tracked by means of drone video footage from a height of 250 m above sea level (Fig. 13) from the moment they entered the sea.

The reconstructed trajectories and drifter velocities made it possible to study the flow structure in the downstream area of the Kodor plume. When the river entered the sea, a laminar flow formed [18, 19], causing the drifters to follow a single trajectory in the direction of the original river flow. At a distance of 50–60 m from the mouth, the laminar flow began to slow and expand, illustrated by the divergence of drifter trajectories. Further uniform deceleration of this flow led to its disappearance 150 m from the river mouth during the first launch and 200 m during the second launch. During both launchesm the drifter velocities were almost the same and decreased from 2.4–2.6 m/s at the delta channel mouth to 0.6–0.8 m/s in the laminar flow dissipation zone. Thus, in case of weak wind action, the spatial scale of the downstream part of the plume, i.e., the part where the inertia of the inflowing river jet is preserved, was 150–200 m. After the final dissipation of the river jet's inertia, the drifters changed direction sharply and synchronously several times within 1–2 min under the influence of wind. Nonlaminar jet drifters also exhibited a greater variabil-

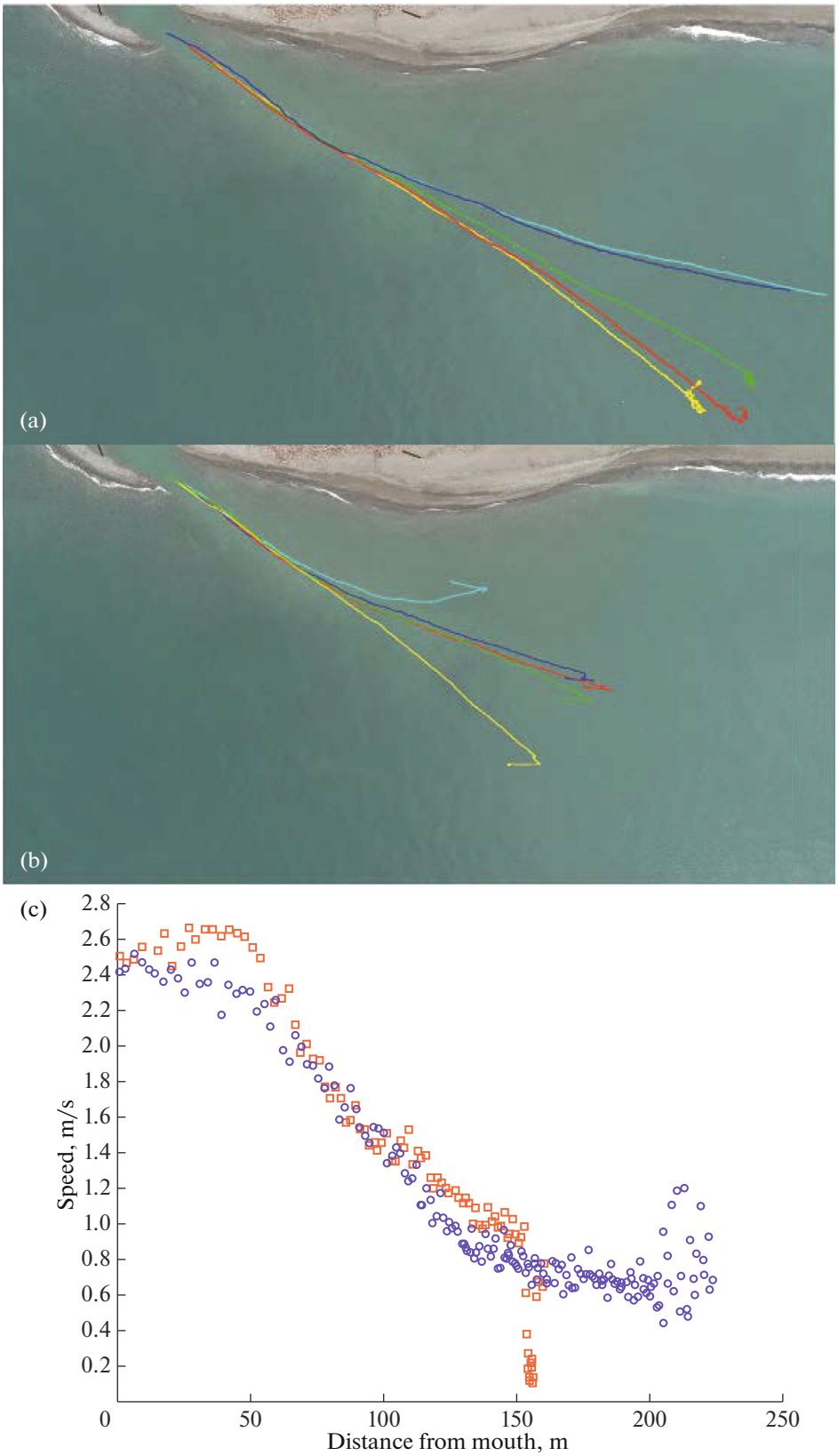

Fig. 13. Drifter trajectories in adjacent part of Kodor plume on first (a) and second (b) launches on April 4, 2019. Average velocity of drifters during first (blue circles) and second (red squares) launches (c).

ity from 0.1 to 0.8 m/s during the first run and from 0.4 to 1.2 m/s during the second.

3. DISCUSSION

Measurements of the thermochaline structure of the Kodor plume have shown that it is characterized by abnormally low surface salinity compared to other small river plumes in the region under study. The thickness of the plume, in turn, does not exceed 2.5 m even in the adjacent zone, except for narrow frontal zones between the plume and seawater, where the plume thickness can reach 5–6 m as a result of convergence. Thus, the Kodor plume forms a relatively thin stratified layer and thus spreads over a larger area than the Mzymta plume under similar external conditions. This is apparently due to differences in the morphology and hydrological characteristics of the Mzymta and Kodor rivers. The Mzymta River has one deep and wide channel, and as a result, when it flows into the sea, the river runoff mixes more intensively with the underlying seawater and forms a less stratified, deeper, and thus smaller plume than the Kodor, which is formed by the inflow of several relatively small delta tributaries.

Field measurements and drone photographs showed a large number of complex and dynamically active frontal zones inside the Kodor plume. Sharp diurnal and semidiunal fluctuations in river runoff characteristic of small mountain rivers, of which the Kodor is one, result in great variability in the size of the Kodor plume at specific times. In particular, during short-term rainfall, the area of the studied plume can change several times in 1–2 days, which was documented during the expeditionary research. Because of this, the previously formed and undissipated residual plume has significantly different thermochaline and dynamic characteristics with the new plume, which leads to the formation of a complex system of internal fronts. Thus, in addition to the variability of wind conditions, fluctuations in river runoff have a very significant impact on the structure and dynamics of the Kodor plume on the diurnal and semidiurnal time scales. In addition, the Kodor plume had clear internal fronts that formed when dynamically active parts of the plumes flowed around shoals. Another important factor in the formation of internal fronts in the studied plume is the presence of several close-lying and large delta branches, which serve as sources of freshwater runoff into the sea. As a result, the plume areas formed by different delta branches also interact with each other as different water masses.

Circulation studies of the Kodor plume have shown significant differences between its dynamics and that of the surrounding seawater. The eddy formation and dissipation in the plume and the subsequent formation, propagation, and dissipation of internal waves from the outer boundary of this eddy were recorded by the drone. A drift experiment in the near-surface area of the plume recorded a slowing the fast river flow (2.5 m/s) into the sea due to its lateral expansion and friction with the underlying seawater. It was found that the inertial part of the Kodor plume is relatively small (150–200 m), which does not result in anticyclonic circulation (a "bulge") in the near-surface part of the plume [16, 20, 29, 51], typical of large river plumes under low wind action. After the inertia of the inflowing river jet dissipates, the drifter trajectories show that the plume velocity and direction respond very quickly (in less than 1 min) to wind action, which is also atypical of large river plumes [13, 15, 22, 50].

The Kodor River has a high flow velocity (2.5 m/s), but the delta channels are relatively shallow (about 1 m). Because of this, the river jet flowing into the sea has a high velocity, but small vertical scale and volume, which causes its inertia to dissipate rapidly. As a result, the spatial scale of the inertial part of the Kodor plume is an order of magnitude smaller than that of rivers with similar flow volumes but lower flow velocities [44, 45, 54]. The spatial scale of the inertial part of the Kodor plume is also an order of magnitude smaller than predicted by the existing parameterization of the scale of the inertial part of the plume based on the characteristics of incoming river runoff based on the Burger and Rossby numbers [20, 51]. The small scale of the inertial part of the plume and absence of anticyclonic circulation in the downstream area significantly affect the structure and dynamics of the river plume. In particular, the runoff of the Kodor River is quickly transported into the area of the plume, the dynamics of which is governed by wind action, which prevents the accumulation of freshwater runoff in the downstream zone described in a number of previous papers [16, 20, 29].

4. CONCLUSIONS

This paper studies the hydrophysical structure and circulation of the Kodor River plume, one of the many small river plumes on the northeastern Black Sea coast. The significant heterogeneity of the small river plume structure is shown, which is caused both by the peculiarities of plume formation by several closely located freshwater runoff sources, which are subjected to sharp fluctuations in river discharge rate, and by interaction of the plume with the regional bottom topography (shoals). Significant spatial scales of the response of circulation in the plume to the variability of wind action on scales of minutes and hours were established. For the first time, field measurements and aerial photography recorded the formation and dissipation of the eddy inside the plume, the generation of internal waves at the plume boundary, and their subsequent propagation and dissipation. For the first time, numerical characteristics of the velocity of such internal waves were obtained. Circulation in the near-surface zone of a small plume has been studied; small spatial scales of the inertial zone of the plume have been established. The absence of anticyclonic circulation in

the downstream part of the plume under weak wind action has been demonstrated.

The results obtained in this study are important for understanding the general aspects of the structure and dynamics of small river plumes, which remain largely unexplored. Most previous studies on river plumes considered those formed by large rivers, while small river plumes received much less attention. This seems to be due to the relatively small impact of individual small river plumes on the coastal zone compared to large plumes. Nevertheless, the total share of small rivers in global freshwater and solid continental runoff is estimated at 25 and 40%, respectively [28]. In many coastal regions of the world, the total contribution of small rivers to total continental runoff can equal or exceed that of large rivers [23, 46, 49].

FUNDING

The study was supported by the Ministry of Science and Higher Education of the Russian Federation, topic no. 0149-2019-0003 (field data collection) and project 14.W03.31.0006 (field data processing), as well as by the Russian Science Foundation, project no. 18-17-00156 (river plume study).

REFERENCES

1. *Water Resources of the Caucasus*, Ed. by G. G. Svanidze and V. Sh. Tsomaya (Gidrometeoizdat, Leningrad, 1988) [in Russian].
2. Sh. Dzhaoshvili, *River Sediment and Beach Formation on the Black Sea Coast of Georgia* (Sabchota Sakartvelo, Tbilisi, 1986) [in Russian].
3. Sh. Dzhaoshvili, Rivers of the Black Sea: Technical report no. 71, European Environmental Agency, 2002. http://www.eea.europa.eu/ru/publications/technical_report_2002_71/at_download/file.
4. P. O. Zavialov, A. S. Izhitskiy, A. A. Osadchiev, et al., "The structure of thermohaline and bio-optical fields in the surface layer of the Kara Sea in September 2011," Oceanology (Engl. Transl.) **55**, 461–471 (2015).
5. P. O. Zavialov, P. N. Makkaveev, B. V. Konovalov, et al., "Hydrophysical and hydrochemical characteristics of the sea areas adjacent to the estuaries of small rivers of the Russian coast of the Black Sea," Oceanology (Engl. Transl.) **54**, 265–280 (2014).
6. O. A. Korotkina, P. O. Zavialov, and A. A. Osadchiev, "Submesoscale variability of the current and wind fields in the coastal region of Sochi," Oceanology (Engl. Transl.) **51**, 745–754 (2011).
7. O. A. Korotkina, P. O. Zavialov, and A. A. Osadchiev, "Synoptic variability of currents in the coastal waters of Sochi," Oceanology (Engl. Transl.) **54**, 545–556 (2014).
8. N. M. Mingazova, R. S. Dbar, V. M. Ivanova, et al., "The state of estuarine areas of the rivers of the Republic of Abkhazia and their impact on the Black Sea coast," Morsk. Biol. Zh. **1** (4), 30–39 (2016).
9. A. A. Osadchiev, "Spreading of the Amur River plume in the Amur Liman, Sakhalin Gulf, and the Strait of Tartary," Oceanology (Engl. Transl.) **57**, 376–382 (2017).
10. A. A. Polukhin, A. D. Zagovenkova, P. V. Khlebopashev, et al., Okeanologiya (Moscow) (in press).
11. Ya. A. Ekba, R. S. Dbar, and A. K. Akhsalba, "Climate change trends in the Southwestern Caucasus in the 20th century," in *Proceedings of the International Scientific-Practical Conference "Biosphere and a Man"* (Maikop, 2003), pp. 38–41.
12. Ya. A. Ekba, R. S. Dbar, and A. K. Akhsalba, "Regional climatic changes and environmental problems in Abkhazia," Ustoich. Razvit. Gorn. Territ. **7** (4), 42–52 (2015).
13. B.-J. Choi and J. L. Wilkin, "The effect of wind on the dispersal of the Hudson River plume," J. Phys. Oceanogr. **37**, 1878–1897 (2007).
14. C. Denamiel, W. P. Budgell, and R. Toumi, "The Congo River plume: Impact of the forcing on the far field and near field dynamics," J. Geophys. Res.: Oceans **118**, 964–989 (2013).
15. D. A. Fong and W. R. Geyer, "Response of a river plume during an upwelling favorable wind event," J. Geophys. Res.: Oceans **106**, 1067–1084 (2001).
16. D. A. Fong and W. R. Geyer, "The alongshore transport of freshwater in a surface-trapped river plume," J. Phys. Oceanogr. **32**, 957–972 (2002).
17. W. R. Geyer, R. C. Beardsley, S. J. Lentz, et al., "Physical oceanography of the Amazon shelf," Cont. Shelf Res. **16**, 575–616 (1996).
18. R. D. Hetland, "Relating river plume structure to vertical mixing," J. Phys. Oceanogr. **5**, 1667–1688 (2005).
19. R. D. Hetland, "The effects of mixing and spreading on density in near-field river plumes," Dyn. Atmos. Oceans **49**, 37–53 (2010).
20. A. R. Horner-Devine, D. A. Fong, S. G. Monismith, et al., "Laboratory experiments simulating a coastal river discharge," J. Fluid Mech. **555**, 203–232 (2006).
21. A. R. Horner-Devine, R. D. Hetland, and D. G. MacDonald, "Mixing and transport in coastal river plumes," Annu. Rev. Fluid Mech. **47**, 569–594 (2015).
22. J. T. Jurisa and R. Chant, "The coupled Hudson River estuarine-plume response to variable wind and river forcings," Ocean Dyn. **62**, 771–784 (2012).
23. T. A. Kniskern, J. A. Warrick, K. L. Farnsworth, et al., "Coherence of river and ocean conditions along the US West Coast during storms," Cont. Shelf Res. **31**, 789–805 (2011).
24. K. A. Korotenko, A. A. Osadchiev, P. O. Zavialov, et al., "Effects of bottom topography on dynamics of river discharges in tidal regions: case study of twin plumes in Taiwan Strait," Ocean Sci. **10**, 865–879 (2014).
25. S. J. Lentz, S. Elgar, and R. T. Guza, "Observations of the flow field near the nose of a buoyant coastal current," J. Phys. Oceanogr. **33**, 933–943 (2003).
26. D. A. Luketina and J. Imberger, "Characteristics of a surface buoyant jet," J. Geophys. Res.: Oceans **92**, 5435–5447 (1987).
27. I. K. Marchevsky, A. A. Osadchiev, and A. Y. Popov, "Numerical modeling of high-frequency internal waves

generated by river discharge in coastal ocean," in *Proceedings of the 5th International Conference on Geographical Information Systems Theory, Applications and Management (GISTAM 2019)* (Heraklion, 2019), pp. 384–387.

28. J. D. Milliman, K. L. Farnsworth, and C. S. Albertin, "Flux and fate of fluvial sediments leaving large islands in the East Indies," J. Sea Res. **41**, 97–107 (1999).
29. D. Nof and T. Pichevin, "The ballooning of outflows," J. Phys. Oceanogr. **31**, 3045–3058 (2001).
30. J. O'Donnell, G. O. Marmorino, and C. L. Trump, "Convergence and downwelling at a river plume front," J. Phys. Oceanogr. **28**, 1481–1495 (1998).
31. A. A. Osadchiev, "A method for quantifying freshwater discharge rates from satellite observations and Lagrangian numerical modeling of river plumes," Environ. Res. Lett. **10**, 085009 (2015).
32. A. A. Osadchiev, "Estimation of river discharge based on remote sensing of a river plume," Proc. SPIE **9638**, 96380H (2015).
33. A. A. Osadchiev, "Small mountainous rivers generate high-frequency internal waves in coastal ocean," Sci. Rep. **8**, 16609 (2018).
34. A. A. Osadchiev, E. E. Asadulin, A. Yu. Miroshnikov, et al., "Bottom sediments reveal inter-annual variability of interaction between the Ob and Yenisei plumes in the Kara Sea," Sci. Rep. **9**, 18642 (2019).
35. A. A. Osadchiev, A. S. Izhitskiy, P. O. Zavialov, et al., "Structure of the buoyant plume formed by Ob and Yenisei river discharge in the southern part of the Kara Sea during summer and autumn," J. Geophys. Res.: Oceans **122**, 5916–5935 (2017).
36. A. A. Osadchiev, K. A. Korotenko, P. O. Zavialov, et al., "Transport and bottom accumulation of fine river sediments under typhoon conditions and associated submarine landslides: case study of the Peinan River, Taiwan," Nat. Hazards Earth Syst. Sci. **16**, 41–54 (2016).
37. A. A. Osadchiev and E. A. Korshenko, "Small river plumes off the north-eastern coast of the Black Sea under average climatic and flooding discharge conditions," Ocean Sci. **13**, 465–482 (2017).
38. A. A. Osadchiev, I. P. Medvedev, S. A. Shchuka, et al., "Influence of estuarine tidal mixing on structure and spatial scales of large river plumes," Ocean Sci. **16**, 1–18 (2020).
39. A. A. Osadchiev, M. N. Pisareva, E. A. Spivak, et al., Freshwater transport between the Kara, Laptev, and East-Siberian seas," Sci. Rep. **10**, 13041 (2020).
40. A. A. Osadchiev and R. O. Sedakov, "Spreading dynamics of small river plumes off the northeastern coast of the Black Sea observed by Landsat 8 and Sentinel-2," Remote Sens. Environ. **221**, 522–533 (2019).
41. A. A. Osadchiev, K. P. Silvestrova, and S. A. Myslenkov, "Wind-driven coastal upwelling near large river deltas in the Laptev and East-Siberian seas," Remote Sens. **12**, 844 (2020).
42. A. A. Osadchiev and P. O. Zavialov, "Lagrangian model of a surface-advected river plume," Cont. Shelf Res. **58**, 96–106 (2013).
43. A. A. Osadchiev and P. O. Zavialov, "Structure and dynamics of plumes generated by small rivers," in *Estuaries and Coastal Zones: Dynamics and Response to Environmental Changes*, Ed. by J. Pan (InTechOpen, London, 2020), Chap. 5, pp. 125–144.
44. C. E. Ostrander, M. A. McManus, E. H. DeCarlo, et al., "Temporal and spatial variability of freshwater plumes in a semi-enclosed estuarine–bay system," Estuaries Coasts **31**, 192–203 (2008).
45. L. Romero, D. A. Siegel, J. C. McWilliams, et al., "Characterizing storm water dispersion and dilution from small coastal streams," J. Geophys. Res.: Oceans **121**, 3926–3943 (2016).
46. G. S. Saldias, J. L. Largier, R. Mendes, et al., "Satellite-measured interannual variability of turbid river plumes off central-southern Chile: spatial patterns and the influence of climate variability," Progr. Oceanogr. **146**, 212–222 (2016).
47. R. V. Schiller, V. H. Kourafalou, P. Hogan, et al., "The dynamics of the Mississippi River plume: impact of topography, wind and offshore forcing on the fate of plume waters," J. Geophys. Res.: Oceans **116**, C06029 (2011).
48. J. H. Simpson, "Physical processes in the ROFI regime," J. Mar. Sys. **12**, 3–15 (1997).
49. R. A. Wheatcroft, M. A. Goni, J. A. Hatten, et al., "The role of effective discharge in the ocean delivery of particulate organic carbon by small, mountainous river systems," Limnol. Oceanogr. **55**, 161–171 (2010).
50. M. M. Whitney and R. W. Garvine, "Wind influence on a coastal buoyant outflow," J. Geophys. Res.: Oceans **110**, C03014 (2005).
51. A. E. Yankovsky and D. C. Chapman, "A simple theory for the fate of buoyant coastal discharges," J. Phys. Oceanogr. **27** (7), 1386–1401 (1997).
52. I. B. Zavialov, A. A. Osadchiev, R. O. Sedakov, et al., "Water exchange between the Sea of Azov and the Black Sea through the Kerch Strait," Ocean Sci. **16**, 15–30 (2020).
53. P. O. Zavialov, V. V. Pelevin, N. A. Belyaev, et al., "High resolution LiDAR measurements reveal fine internal structure and variability of sediment-carrying coastal plume," Estuarine, Coastal Shelf Sci. **205**, 40–45 (2018).
54. J. Zhao, W. Gong, and J. Shen, "The effect of wind on the dispersal of a tropical small river plume," Front. Earth Sci. **12**, 170–190 (2018).